9-20-2023

Designing polymers for cartilage uptake: effects of architecture and molar mass.

Jue Gong

Jordan Nhan

Jean-Philippe St-Pierre

Elizabeth R Gillies

ARTICLE

Designing Polymers for Cartilage Uptake: Effects of Architecture and Molar Mass

Received 00th January 20xx,
Accepted 00th January 20xx

DOI: 10.1039/x0xx00000x

Jue Gong,[a] Jordan Nhan,[b] Jean-Philippe St-Pierre*[b] and Elizabeth R. Gillies*[a,c]

Osteoarthritis (OA) is a progressive disease, involving the progressive breakdown of cartilage, as well as changes to the synovium, and bone. There are currently no disease-modifying treatments available clinically. An increasing understanding of the disease pathophysiology is leading to new potential therapeutics, but improved approaches are needed to deliver these drugs, particularly to cartilage tissue, which is avascular and contains a dense matrix of collagens and negatively charged aggrecan proteoglycans. Cationic delivery vehicles have been shown to effectively penetrate cartilage, but these studies have thus far largely focused on proteins or nanoparticles, and the effects of macromolecular architectures have not yet been explored. Described here is the synthesis of a small library of polycations composed of *N*-(2-hydroxypropyl)methacrylamide (HPMA) and *N*-(3-aminopropyl)methacrylamide (APMA) with linear, 4-arm, or 8-arm structures and varying degrees of polymerization (DP) by reversible addition fragmentation chain-transfer (RAFT) polymerization. Uptake and retention of the polycations in bovine articular cartilage was assessed. While all polycations penetrated cartilage, uptake and retention generally increased with DP before decreasing for the highest DP. In addition, uptake and retention were higher for the linear polycations compared to the 4-arm and 8-arm polycations. In general, the polycations were well tolerated by bovine chondrocytes, but the highest DP polycations imparted greater cytotoxicity. Overall, this study reveals that linear polymer architectures may be more favorable for binding to the cartilage matrix and that the DP can be tuned to maximize uptake while minimizing cytotoxicity.

Introduction

Osteoarthritis (OA) is a leading cause of chronic disability globally, reducing mobility, independence, and quality of life for affected patients.[1, 2] It is a progressive disease, involving the breakdown of cartilage, inflammation of the synovium, and changes to the subchondral bone.[3] Initial interventions are typically conservative in nature and include treatments aimed at relieving pain, notably by prescribing systemic analgesics or nonsteroidal anti-inflammatory drugs.[4] Additional options include the intra-articular injection of corticosteroids[5] or hyaluronic acid[6]; however, these treatments only aim to temporarily relieve symptoms and there are currently no disease-modifying treatments approved by regulatory bodies to stop, or reverse the progression of OA. As such, joint replacement surgeries are often needed to treat end-stage OA, when conservative treatments are no longer effective.[7, 8]

For years, a significant barrier to the development of disease-modifying OA therapeutics was a poor understanding of the molecular mechanisms involved in OA. However, understanding of the complex disease pathophysiology has been increasing in recent years, leading to new opportunities for OA treatment.[9] As articular cartilage loss is one of the hallmarks of OA progression, cartilage has been an important therapeutic target. For example, inhibitors of matrix metalloproteinases[10] and aggrecanases,[11, 12] which degrade collagen and aggrecan in cartilage respectively, are being studied. Recombinant human fibroblast growth factor 18 is also being investigated as a promoter of cartilage repair.[13] However, the potential therapeutics that have undergone clinical trials thus far have not yet succeeded due in part to issues such as adverse effects and poor therapeutic efficacy.[10-12, 14] Intra-articular delivery is a promising approach to mitigate the side effects associated with systemic administration and enhance efficacy by delivering the correct dose of a drug to the target tissue.[15-17] However, the rapid clearance of drugs from the joint space,[18, 19] combined with the avascular nature of cartilage and its dense anionic network of collagen and aggrecan proteoglycans makes it difficult for therapeutics to reach targets, such as chondrocytes embedded within cartilage.[20, 21] Various delivery systems such as nano- and microparticles,[22, 23] as well as hydrogels[24, 25] have been investigated to reduce the clearance rate of drugs from the joint, but larger particles and hydrogels do not typically enable the delivery of therapeutics into cartilage and rely on diffusion of the therapeutic from the synovial fluid through the tissue.[20, 26] These strategies also do not fully resolve issues with rapid joint clearance.

[a] *Department of Chemistry, The University of Western Ontario, 1151 Richmond St., London, Ontario, Canada, N6A 5B7.*
[b] *Department of Chemical and Biological Engineering, University of Ottawa, 161 Louis-Pasteur Pvt., Ottawa, Ontario, Canada, K1N 6N5.*
[c] *Department of Chemical and Biochemical Engineering, The University of Western Ontario, 1151 Richmond St., London, Ontario, Canada, N6A 5B9.*
*Email: Jean-Philippe.St-Pierre@uOttawa.ca; egillie@uwo.ca
Electronic Supplementary Information (ESI) available: [details of any supplementary information available should be included here]. See DOI: 10.1039/x0xx00000x

Several groups have reported cartilage-penetrating drug delivery systems, whereby carrier design focused on generating sufficiently small materials for entry and diffusion into the dense extracellular matrix (ECM) of the tissue. For example, poly(ethylene glycol) (PEG)-modified single-walled carbon nanotubes with diameters less than 10 nm and lengths from tens to hundreds of nm were shown to deliver antisense oligonucleotides to chondrocytes in the cartilage of healthy and OA mice after intra-articular injection.[27] Phage display technology was used to develop peptides that bind to type II collagen[28] or chondrocytes[29] in cartilage. The conjugation of these peptides to drug carriers such as small Pluronic F-127 nanoparticles,[28] lipid-polymer hybrid particles,[30] or a polyethylenimine non-viral transfection agent[29] enhanced the penetration of these delivery systems into cartilage.

Cartilage penetration approaches have also exploited electrostatic interactions between the delivery system and the anionic cartilage matrix.[31] For example, avidin, a 7 nm diameter cationic protein was found to more effectively penetrate cartilage explants compared to neutral avidin analogues.[31] Uptake and enhanced half-lives of cationic avidin were also observed in rat and rabbit joints.[32, 33] Recently, avidin functionalized with multiple 8-arm amino-terminated PEG chains was also investigated, with the PEG chains providing multiple sites for drug conjugation and delivery into cartilage.[34, 35] Engineered green fluorescent proteins were explored to demonstrate that optimization of the charge density was necessary to balance binding to and transport through cartilage.[36] In addition, a study using polyelectrolyte complexes of insulin-like growth factor 1 (IGF-1) found that a larger number of surface cationic charges led to increased binding to explanted bovine cartilage, although some degree of PEGylation was necessary to mitigate cytotoxicity.[37] Cationic polyamidoamine (PAMAM) dendrimers were also used for the delivery of IGF-1 into cartilage and treatment of OA in a rat model.[38] Tuning of the dendrimer generation and degrees of peripheral PEGylation allowed for the toxicity, uptake, and retention of the dendrimer-IGF-1 conjugate to be optimized. Furthermore, cationic 20-mer peptide carriers with varying numbers and arrangements of cationic charges were explored to determine the optimal number and sequence of charges for cartilage uptake.[39] While much effort has been undertaken to study the role of overall charge and charge distribution in cationic cartilage-penetrating carriers, to the best of our knowledge, efforts have not been directed to understanding the role of macromolecular architecture of cationic carriers in cartilage uptake, even though it is likely to impact both diffusion through and binding to the ECM.

Here, we present the synthesis and study of a small library of cationic synthetic polymers with varying chain length and architecture to examine the effect of these properties on cartilage uptake and retention (Fig. 1). The preparation of chain transfer agents for the synthesis of linear, 4-arm, and 8-arm polycations is described, followed by chain extension via reversible addition fragmentation chain-transfer (RAFT) polymerization with the monomers *N*-(2-hydroxypropyl)methacrylamide (HPMA) and *tert*-butyl carbamate protected *N*-(3-aminopropyl)methacrylamide (Boc-APMA) to balance cationic and neutral hydrophilic pendant groups on the polymers following Boc deprotection. Uptake into freshly explanted bovine articular cartilage and cytotoxicity in bovine chondrocytes is explored, revealing important trends with respect to molar mass and architecture that should be considered in the design of cartilage delivery systems.

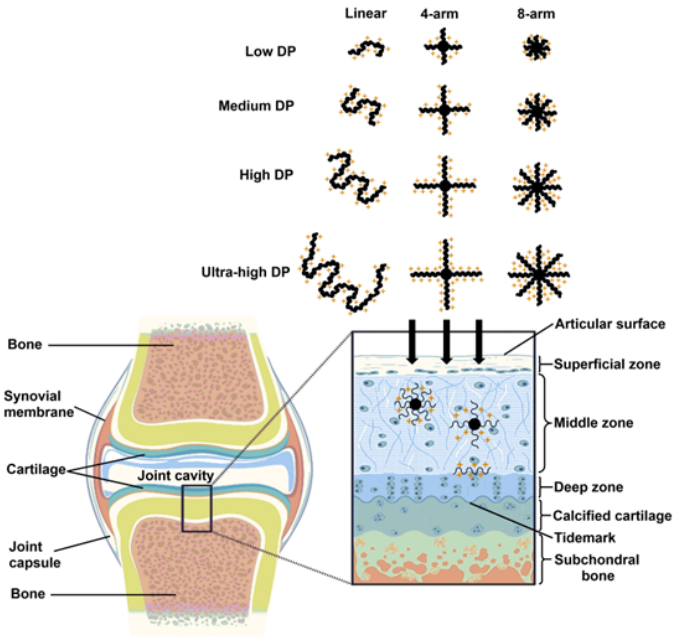

Fig. 1 Schematic representation of the study design, which involves the synthesis of polycations with varying degree of polymerization (DP) and architectures for investigation of their penetration into and retention in articular cartilage tissue.

Results and discussion

Synthesis of chain transfer agents

Multi-arm polymers can be synthesized using arm-first or core-first techniques, or a combination of both.[40] The arm-first technique couples multiple linear polymers to a multifunctional core. However, it can be difficult to control the dispersity and number of arms on the resulting polymer using this approach.[40] Therefore, in addition to linear polymers, a core-first approach employing multifunctional cores to grow the polymers with 4 or 8 arms was used in this study. RAFT was selected as a versatile and controlled radical polymerization method.[41] RAFT polymerization employs chain transfer agents (CTAs) in the form of thiocarbonylthio compounds. For the current work, dithiobenzoate-based RAFT agents were selected as they are suitable for the polymerization of methacrylamide monomers.[42] Thus, to prepare linear, 4-arm, and 8-arm polycations, three different dithiobenzoate-based CTAs were synthesized (Fig. 2). For preparation of the linear polymers, 4-cyanopentanoic acid dithiobenzoate (CTP) was synthesized as previously reported.[43]

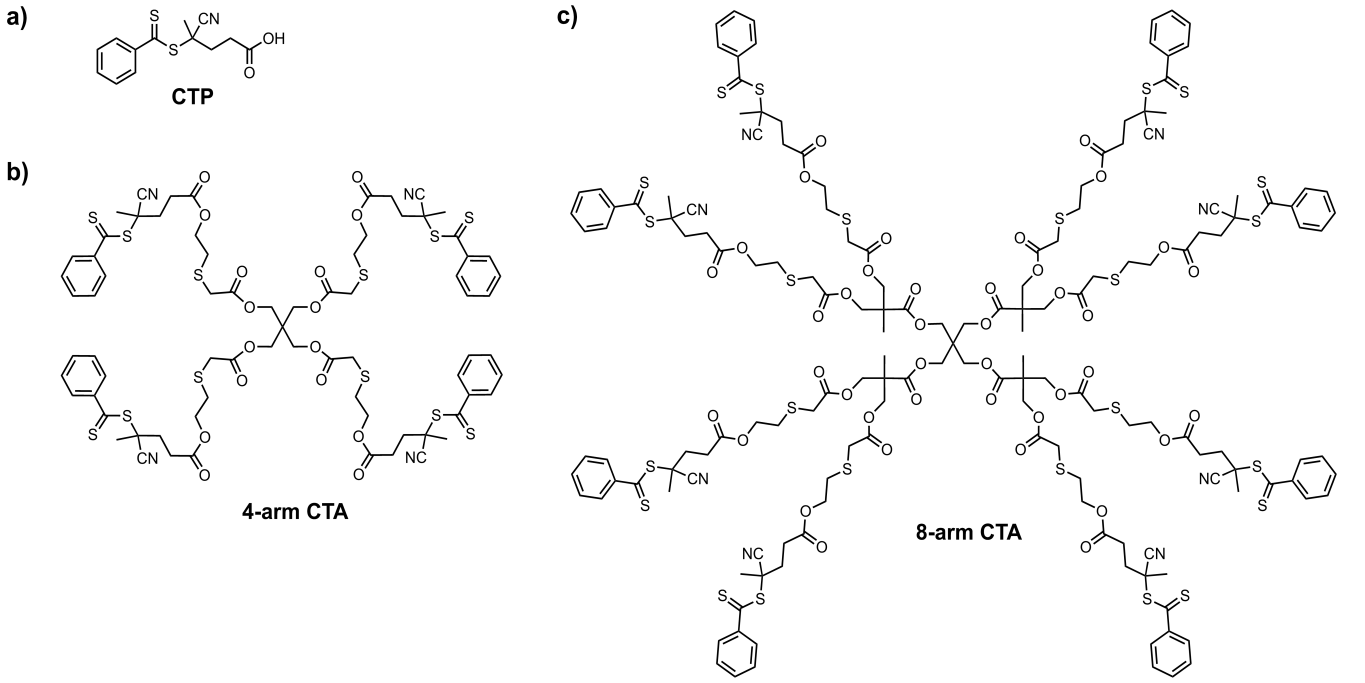

Fig. 2 Structures of (a) CTP; (b) 4-arm CTA; (c) 8-arm CTA.

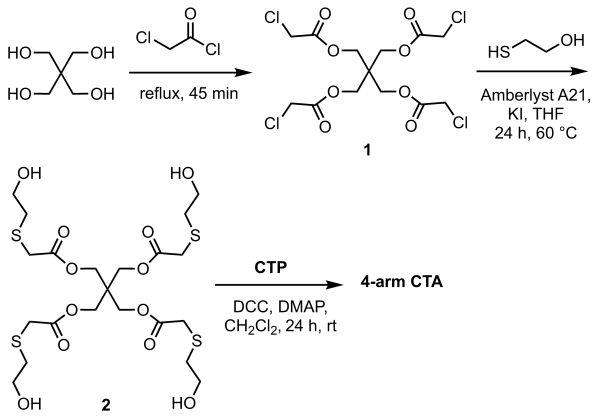

Scheme 1 Synthesis of the 4-arm CTA.

The 4-arm CTA comprised CTP conjugated to pentaerythritol with a thioether spacer. The spacer was necessary, as attempts to directly conjugate CTP to pentaerythritol were unsuccessful. The synthesis of the 4-arm CTA first involved the reaction of pentaerythritol with chloroacetyl chloride to yield pentaerythritol tetrachloroacetate (**1**) (Scheme 1). Then, **1** was reacted with 2-mercaptoethanol in the presence of the tertiary amine-functionalized resin Amberlyst™ A-21 and KI as a catalyst to produce the tetraol **2**. It has been reported that the introduction of a thioether group in the α-position relative to an ester can slow hydrolytic degradation in comparison with the unmodified ester.[44-46] Finally, the hydroxyl groups on **2** were coupled to CTP using *N*,*N*'-dicyclohexylcarbodiimide (DCC) in the presence of 4-(dimethylamino)pyridine (DMAP) to generate the 4-arm CTA. The structures of the intermediates and products were confirmed by techniques including ^{1}H NMR, ^{13}C NMR, and infrared (IR) spectroscopic methods, as well as high resolution mass spectrometry (Fig. S1-S3, S38-40).

The 8-arm CTA was based on a pentaerythritol core with 2,2-bis(hydroxymethyl)propionic acid (bis-MPA) branching units. First, the two hydroxyls of bis-MPA were esterified by reaction with chloroacetyl chloride to provide compound **3** (Scheme 2).

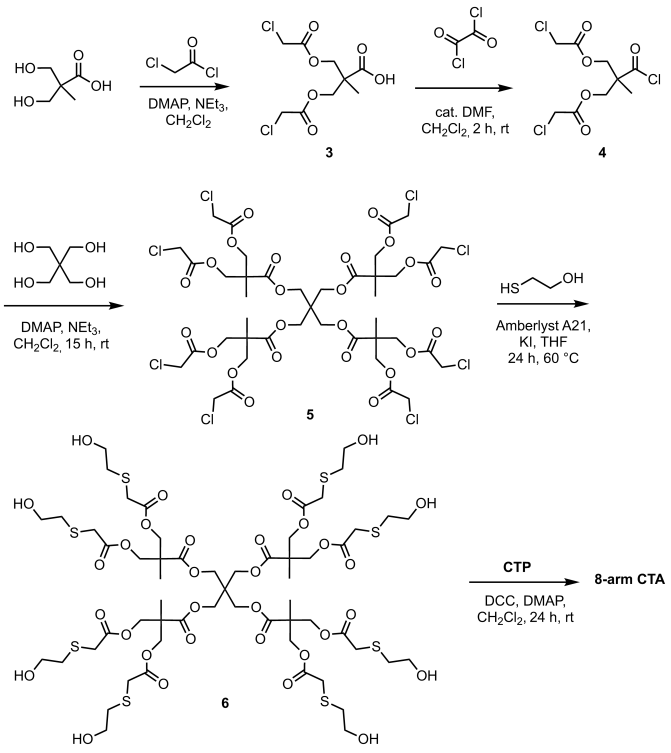

Scheme 2 Synthesis of the 8-arm CTA

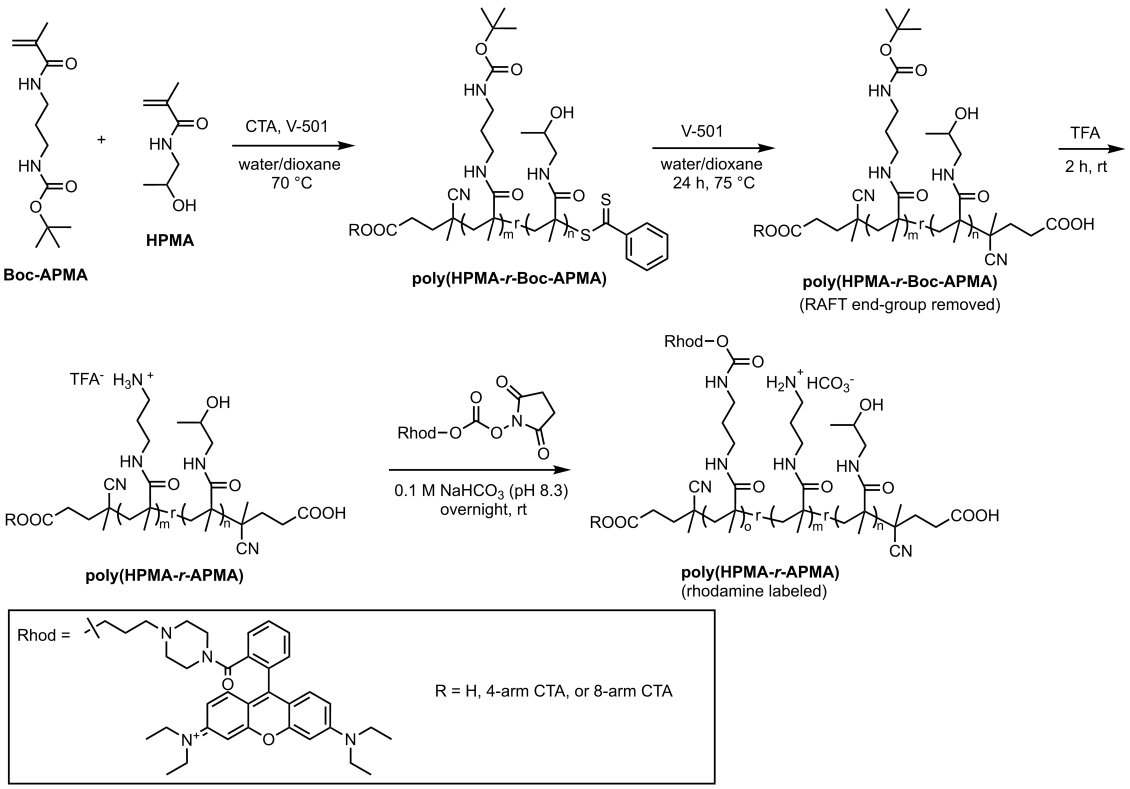

Scheme 3 Synthesis of poly(HPMA-r-Boc-APMA), followed by removal of the terminal dithiobenzoate, Boc protecting groups, and labeling with rhodamine B.

Initially, we attempted to react compound **3** with pentaerythritol using DCC, but the reaction did not proceed to completion, and it was not possible to purify the product. Instead, the carboxylic acid of **3** was converted to a more reactive acid chloride (**4**) using oxalyl chloride, and **4** was then cleanly reacted with pentaerythritol to yield compound **5**. Next, the peripheral chloride moieties on **5** were reacted with 2-mercaptoethanol to produce **6** and the resulting hydroxyls were coupled with CPT to give the final 8-arm CTA as described above for the 4-arm CTA (Fig. S4-S8 and S41-S45).

Polymer Synthesis

We selected a copolymer of HPMA and APMA as the cationic polymer. Poly(HPMA) is well established as a water-soluble polymer that is well tolerated in drug delivery applications.[47-49] In addition, Kleinberger et al. previously synthesized a series of APMA/HPMA random copolymers with four different APMA percentages (10, 25, 50 and 75 mol% APMA) using RAFT polymerization and found that polycations with lower APMA content (10 and 25 mol% APMA) gave better cytocompatibility.[50] We postulated that polycations with the lowest charge density (10 mol% APMA) would not exhibit sufficient positive charge density to bind effectively to and penetrate cartilage, and we therefore selected 25% APMA for this study. Although APMA has been previously polymerized using RAFT,[50, 51] we prepared and polymerized the *t*-butyloxycarbonyl protected APMA monomer (Boc-APMA) as we found size exclusion chromatography (SEC) characterization of the polycations problematic due to column adsorption. Preparation of the protected polymers allowed them to be readily characterized in their protected forms before conversion to polycations by deprotection. Boc-APMA[52] and HPMA[53] were synthesized using modified versions of previously reported procedures (Fig. S9-S11).

Copolymerization was performed using Boc-APMA and HPMA to prepare four different degrees of polymerization (DP) for each series of architectures (linear, 4-arm and 8-arm) (Scheme 3). A solvent system consisting of water and dioxane was selected to provide sufficient solubility for both monomers, the CTA, and the resulting polymers. We found that 2:1 water/dioxane (v/v) was suitable for the linear polymers, whereas 1:3 water/dioxane (v/v) was required to dissolve the 4- and 8-arm CTA. The polymerizations were performed at 70 °C using V-501 as the initiator at 25 mol% relative to the dithiobenzoate moiety in each CTA to produce poly(HPMA-*r*-Boc-APMA).

To synthesize linear copolymers, monomer/CTP ratios of 82:1, 170:1, 390:1 and 763:1 were used for the low, medium, high, and ultra-high DPs, corresponding to theoretical number average molar masses (M_n) of 13.9 kg/mol, 28.7 kg/mol, 65.5 kg/mol and 128.2 kg/mol respectively if conversion was 100%. These chain lengths were targeted with the goal to obtain polymers with hydrodynamic diameters ranging from a few nm to more than 10 nm.[54] Based on the previously reported RAFT polymerization of HPMA and Boc-APMA,[55] as well as our own initial experiments, a polymerization time of 17 h was selected. Monomer conversion was determined by comparing the

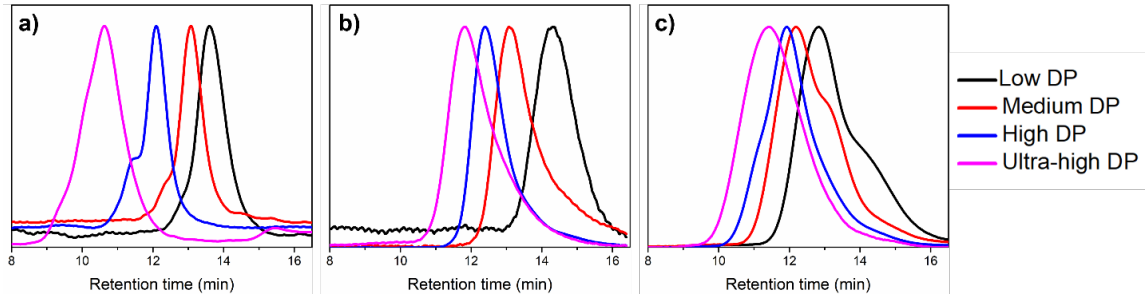

Fig. 3 Overlays of the SEC chromatograms for (a) linear; (b) 4-arm; (c) 8-arm poly(HPMA-r-Boc-APMA), using refractive index detection.

integrals of the monomer alkene peaks at 5.6 and 5.4 ppm to the peak at 3.2 – 2.9 ppm corresponding to methylene protons from both monomers and polymers in ^{1}H NMR spectra (Fig. S12). A conversion of 83% was
obtained for the low DP copolymer while the medium, high, and ultra-high DP copolymers had conversions of 65%, 73% and 70% respectively. The resulting copolymers were purified by precipitation in acetone, and characterized by ^{1}H NMR spectroscopy, IR spectroscopy and SEC. ^{1}H NMR spectroscopy confirmed the incorporation of both monomers into the copolymers (Fig. S13-S16). Comparing the integrals of the peak at 3.8 ppm corresponding to the methine proton adjacent to the alcohol in the 2-hydroxypropyl unit with the integral of the peak at 1.4 ppm corresponding to the Boc methyl groups, it was confirmed that the HPMA and APMA monomers were incorporated into the copolymers in a ~3:1 ratio. IR spectroscopy showed characteristic carbonyl peaks at ~1635 and 1520 cm^{-1} as well as a broad peak at ~3340 cm^{-1} attributed to the O-H and N-H stretching. The M_n was determined by ^{1}H NMR spectroscopy based on end-group analysis (Fig. S13-S16), as well as SEC in DMF relative to poly(methyl methacrylate) standards (Table 1, Fig. 3a). The SEC data were in reasonable agreement with the NMR analyses and the dispersities ($Đ$) ranged from 1.19 – 1.53. The ultra-high DP linear polymer had a somewhat elevated M_n and $Đ$, which can likely be attributed to a small degree of chain-chain coupling.[56]

To prepare 4-arm and 8-arm copolymers having similar M_n values as the linear series, the reaction conditions developed for linear RAFT polymerization were initially used. However, bimodal molar mass distributions were observed by SEC, presumably due to star-star coupling at higher conversions. Star-star coupling can be problematic in RAFT polymerization when a core-first technique is used because the propagating radicals are located at the ends of each arm where they are highly accessible to undergo coupling reactions.[57, 58] To avoid this undesired side reaction, we added higher monomer/initiator ratios and stopped the polymerizations at lower conversions to achieve similar DPs to those of the linear polymers (Fig. S17-S24). The kinetics of the polymerizations for the 4-arm CTA and 8-arm CTA at different monomer/CTA ratios were investigated and it was possible to stop the polymerizations at controlled conversions based on plots of monomer conversion versus time (Fig. S46-S53). Stopping the polymerization at 50 – 70% conversion resulted in a series of 4-arm copolymers with very similar M_n values to the linear series (Table 1) and acceptable $Đ$ values ranging from 1.15 – 1.44 (Fig. 3b). To synthesize sufficiently well-defined 8-arm copolymers, the polymerizations were stopped at lower conversions of ~30% to prevent coupling reactions. These copolymers had similar M_n values and $Đ$ values to the linear and 4-arm series up to the high DP analogue, while the ultra-high DP analogue had a slightly higher M_n (Fig. 3c).

Table 1 Summary of molar mass data for the poly(HPMA-r-Boc-APMA) library.

Architecture	Target DP	M_n (NMR) (kg/mol)	M_n (SEC) (kg/mol)	$Đ$
Linear	Low	10.5	12.5	1.19
	Medium	27.2	22.2	1.13
	High	49.5	50.5	1.24
	Ultra-high	80.0	112	1.53
4-arm	Low	9.4	9.1	1.18
	Medium	26.4	18.3	1.15
	High	50.0	30.0	1.23
	Ultra-high	85.5	86.4	1.44
8-arm	Low	11.8	15.8	1.35
	Medium	21.3	21.9	1.42
	High	43.9	41.2	1.43
	Ultra-high	92.3	80.1	1.62

The dithiobenzoate end-groups remaining on the copolymers after RAFT polymerization are hydrophobic, which can affect the behavior of the resulting polymers in aqueous solutions. Moreover, they can undergo hydrolysis to form thiol end-groups that can be toxic to cells,[59] and can also potentially dimerize through disulfide bond formation. Therefore, the

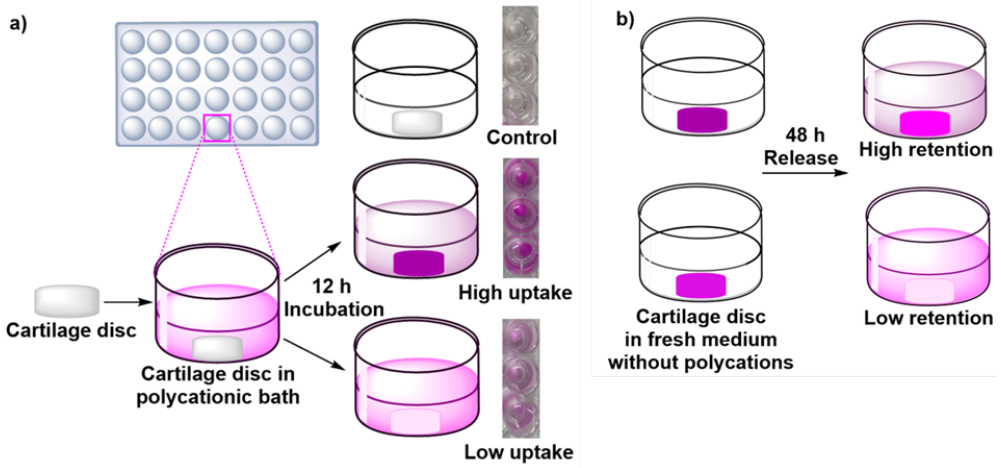

Fig. 4 (a) Schematic showing fluorescently-labeled polycationic polymers uptake into cartilage explants and representative photos showing wells containing cartilage without polycation (control), low uptake of polycation, and high uptake of polycation after 12 h of incubation. (b) Schematic showing cartilage explants incubated in the fresh serum-free medium without polycations for 48 h of release.

dithiobenzoate end-groups were removed by treatment of the copolymers with excess V-501 in 2:1 water/dioxane at 75 °C for 24 h, followed by precipitation in acetone (Scheme 3). The complete removal of the group was confirmed by ^{1}H NMR spectroscopy based on the disappearance of the aromatic peaks from 7.4 – 7.9 ppm (Fig. S25a). In addition, ultraviolet-visible (UV-vis) spectroscopy confirmed the disappearance of the dithiobenzoate absorption at 308 nm (Fig. S25b).

Next, the copolymers were treated with trifluoroacetic acid (TFA) to remove the Boc groups followed by dialysis against deionized water and lyophilization to yield the corresponding polycations (Scheme 3). ^{1}H NMR spectroscopy confirmed the disappearance of the peak at 1.4 ppm corresponding to the Boc methyl protons for all of the polymers (Fig. S26-S37). At this stage, the polymers were also characterized to determine their hydrodynamic diameters and zeta potential. These measurements were performed in 1.5 g/L bicarbonate buffer (pH 7.4), the same buffer system used in the media for the cartilage uptake studies. Dynamic light scattering indicated that the polymers had hydrodynamic diameters from 4 – 17 nm (Fig. S54, Table S2). Within each architectural series, the diameter systematically increased. However, it generally was not possible to elucidate subtle differences in the hydrodynamic diameters across the different architectures due to the challenges in obtaining highly accurate diameter assessments for individually dispersed polymers in solution. The zeta potential generally increased with DP, ranging from +0.3 to +10 mV (Table S2). There were no significant differences between the different architectures.

Finally, the copolymers were labeled with a fluorescent dye to facilitate the quantification of uptake into cartilage. Rhodamine B *N*-hydroxysuccinimide carbonate was prepared as previously reported,[60] and then reacted with the deprotected copolymers in 0.1 M sodium bicarbonate solution (pH 8.3) at a ratio of 0.014 dye equivalents per monomer repeat unit (Scheme 3). Dialysis was subsequently performed to remove any unreacted dye, followed by lyophilization of the polymers. The extent of rhodamine B labeling was quantified by UV-vis spectroscopy, which found that there were 0.2-1.0 dye molecules per 100 repeat units (Table S1). It was assumed that this extent of labeling would be sufficiently low that the dye would not alter polymer uptake in cartilage tissue.

Cartilage uptake and retention

Tissue uptake and retention of the different copolymers synthesized in this study were evaluated in freshly explanted bovine cartilage (Fig. 4a)[36, 38] by incubation in culture medium in the absence or presence of 5% fetal bovine serum (FBS). Uptake was assessed based on the difference between measurements of the fluorescence intensity of rhodamine-labeled polycation solutions incubated with or without cartilage discs for 12 h (Fig. 5a and 5b). This 12 h time point was selected based on the typical retention time of macromolecules in the joint being several hours.[18, 19] Both with and without FBS, there was a trend towards higher uptake with increasing DP (Fig. 5a and 5b). However, for the linear and 8-arm architectures incubated without FBS, and the 8-arm architecture incubated with FBS, the ultra-high DP polycations had lower uptake than their high DP analogues. Meanwhile, for the linear polymers incubated with FBS, uptake was comparable for the two highest DP levels. Comparing the polycations having similar DP but different architectures, the linear polycations consistently had higher uptake than both the 4-arm and 8-arm analogues. In the presence of FBS, uptake was slightly lower for the higher DP polycations. This reduction in uptake can likely be attributed to binding of the polycations to serum proteins such as albumin by hydrophobic and electrostatic interactions, which may increase their size and impact their ability to diffuse through the dense ECM network.[61]

After the initial polycation incubation period, the cartilage explants were transferred to fresh media in the absence of these polymers and incubated for 48 h (Fig. 4b). The fluorescence of the culture media was then measured to quantify the percentage of polycations released from the cartilage and thereby calculate the percentage of polymer remaining in the tissue. In general, polymer retention increased

with DP both in the absence and presence of FBS, with the exception of the ultra-high DP 8-arm polycation, which exhibited lower retention than the lower DP 8-arm analogues both in the presence and absence of FBS (Fig. 5 and S55). When comparing the different architectures, retention was consistently highest for the linear polycations compared to the 4-arm and 8-arm polycations.

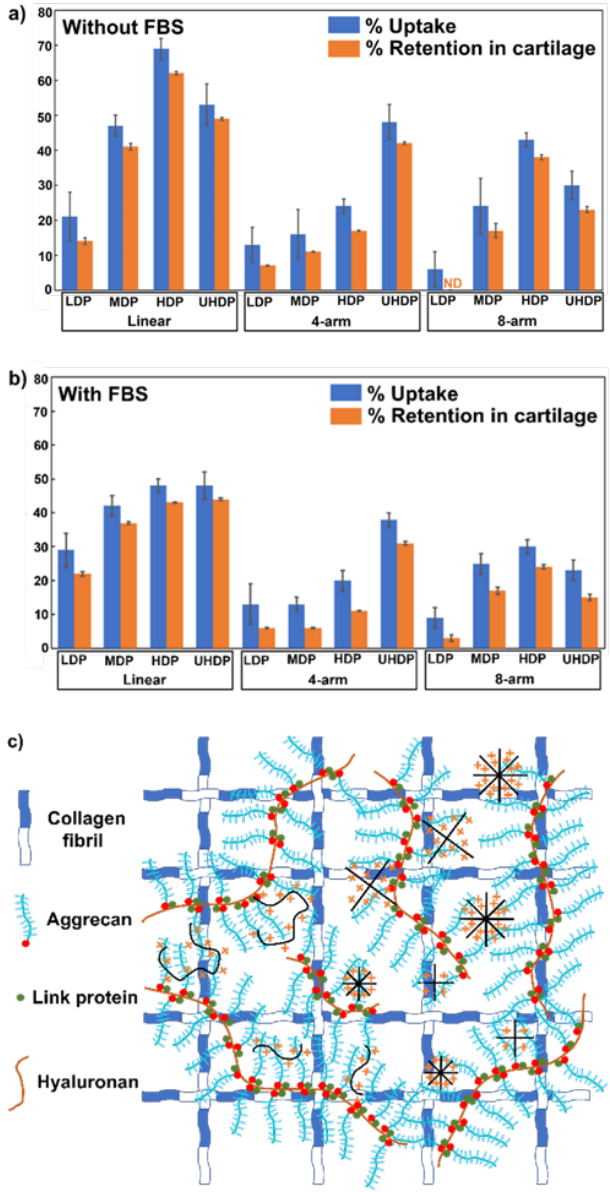

Fig. 5 Polycation uptake (over 12 h) and retention (over 48 h, as a percentage of the initial polycation in solution) in bovine cartilage explants in culture medium (a) without FBS; (b) with 5% FBS; (c) Illustration of interactions between the polycations and aggrecan in cartilage. LDP = low DP; MDP = medium DP; HDP = high DP; UHDP = ultra-high DP; ND = not detected. Error bars correspond to the standard deviation (n = 5 for uptake and n = 3 for retention). Polycation retention as a percentage of uptake is presented in Fig. S54.

We also performed fluorescence microscopy imaging on thin sections of the cartilage explants (Fig. 6, S56 and S57). The distribution of the polycations was quite uniform across the tissue depth, even for the ultra-high DP polycations, with slightly less fluorescence just below the superficial zone, possibly due to lower anionic aggrecan in this region (Fig. S58). The uptake of the polycations into cartilage explants can be influenced by factors that affect their rate of diffusion into the tissue as well as their equilibrium distribution between the cartilage and surrounding media. Previous studies have reported that typically cationic nanocarriers with diameters less than about 15 nm can diffuse into cartilage.[32, 33, 62, 63] Some rigid particles of 15 nm were trapped in the superficial zone.[26] However, in other cases larger polymeric nanoparticles (e.g., 38 nm diameter) were taken up, indicating that a number of complex factors likely govern uptake.[64] While the mesh size of type II collagen has been reported to be 60 – 200 nm,[65] the distance is only 2 – 4 nm between glycosaminoglycan (GAG) chains on aggrecan[66] and the density of aggrecan increases with cartilage depth.[67] Our full library of polymers was able to diffuse throughout the cartilage. These results are consistent with previous reports that avidin, a 66 kDa cationic protein[26] and 6th generation poly(ethylene glycol) (PEG)-functionalized cationic PAMAM dendrimers (58 kDa)[38] were also able to effectively penetrate cartilage. While the molar masses of some of our polymers are higher than 66 kDa and the hydrodynamic diameters of most polycations exceeded 4 nm, it is known that flexible polymers can permeate through pores through an end-on motion in a manner not possible for more globular structures such as proteins and dendrimers.[68-70] It is possible that the 8-arm copolymers may exhibit more globular and less flexible structures than the linear or 4-arm systems, partially explaining the lower uptake of the ultra-high DP 8-arm copolymer compared with the high DP 8-arm copolymer, which is smaller, and the analogous ultra-high DP 4-arm system, which may be more flexible.

Aside from hydrodynamic volume and conformational flexibility, penetration through cartilage can in some cases be hindered by strong electrostatic interactions. For example, while cationic green fluorescent protein variants exhibited higher cartilage uptake than neutral variants, when the charge was increased from +9 to +36, cartilage uptake decreased and was limited in penetration depth.[36] Similar results were also obtained for cationic peptides, where an increase in charge from +8 to +14 resulted in a 7-fold increase in uptake, but further increases in charge to +16 and +20 led to somewhat lower uptake compared to the +14 peptide and the penetration depths were also more limited.[39] In the current study, the cation density remained constant throughout the copolymer library (HPMA:APMA = 3:1). The ability of the copolymers to effectively penetrate the cartilage explants indicates that the necessary dynamic electrostatic binding to allow transport through cartilage was achieved for the selected monomer ratio. However, it is possible that the somewhat lower uptake of the ultra-high DP linear copolymer compared to the high DP linear copolymer (without FBS) can be attributed to hindered diffusion through the cartilage due to its strong bonding and larger hydrodynamic diameter. Such hindrance does not appear to be observed for the analogous ultra-high DP 4-arm system.

Other differences in uptake and retention between the copolymers in our library can likely be attributed to differences

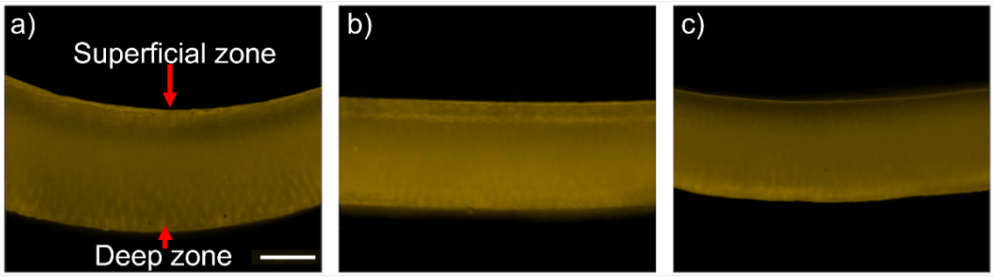

Fig. 6 Fluorescence microscopy images showing cartilage uptake for (a) linear; (b) 4-arm; (c) 8-arm ultra-high DP poly(HPMA-*r*-APMA) in culture medium without FBS. Scale bar = 200 µm. Additional images for other polycations are in the supporting information.

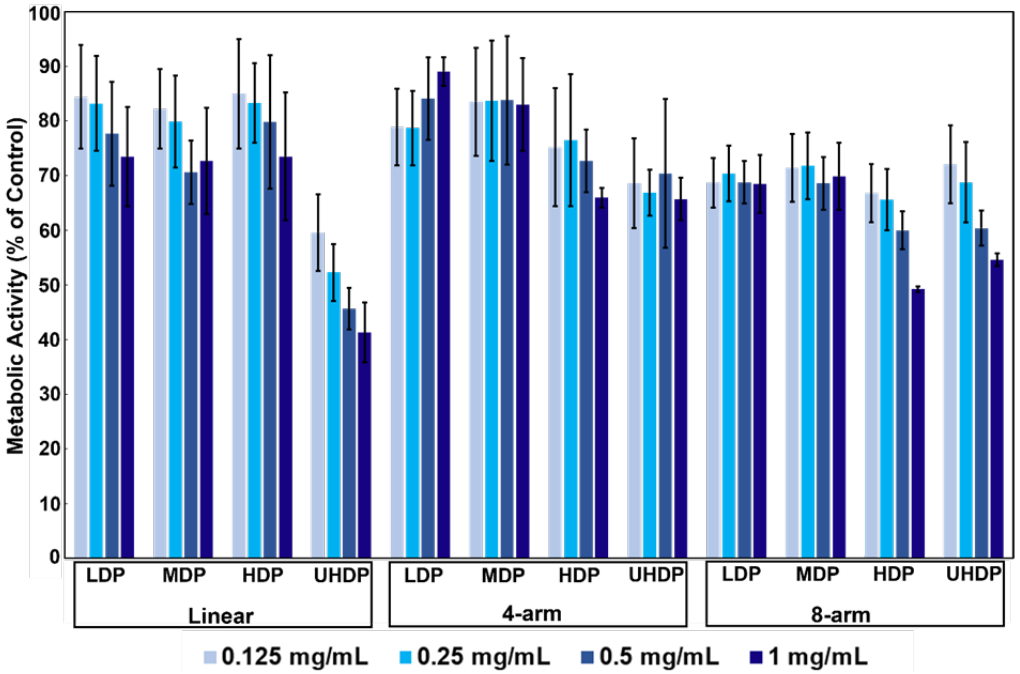

Fig. 7 Cell viability of chondrocytes from excised bovine articular cartilage exposed to varying concentrations of the different polycations. LDP = low DP; MDP = medium DP; HDP = high DP; UHDP = ultra-high DP. Error bars correspond to the standard deviation (n = 3).

in their partitioning between the cartilage and surrounding medium. The number of positive charges was approximately 17, 28, 71, and 134 for the low, medium, high, and ultra-high DP linear copolymers, with similar values for the 4-arm and 8-arm analogues. More charge can lead to stronger binding with negatively charged aggrecan in cartilage. The interaction is not only more enthalpically favorable for polymers having many positive charges, but also more entropically favorable due to the release of many counterions, such as Na^+, from the aggrecan chains. Therefore, the binding of higher molar mass polymers to cartilage should be more favorable, resulting in higher uptake. Aside from the possible differences in diffusion rates noted above, this trend was observed for each architectural series. The generally reduced uptake of the 4-arm and 8-arm copolymers compared to the linear analogues suggests that the star polymer architecture may be less favorable for binding to aggrecan. While linear polymers can undergo conformational changes that maximize electrostatic binding, a portion of the cationic groups in a star polymer may be buried near the core of the molecule and unavailable for binding (Fig. 5c).

A number of factors may influence the direct translation of these findings to human joint cartilage for OA treatment. In the current study, we focused on intact cartilage, as potential OA therapeutics are most likely to be successful in halting or reversing OA progression at an early stage of the disease, before substantial cartilage degradation has occurred.[71] Of course, early intervention would require further advances in our ability to diagnose early-stage OA. A recent study investigated the effect of partial digestion of bovine cartilage explants with collagenase type II (as a model of OA) on nanoparticle uptake.[72] It was found that the tissue digestion impacted uptake differentially depending on the physical properties of the particles, likely because of the opposing effects of increased ECM permeability and decreased fixed-charge density due to proteoglycan depletion. In addition, whereas human articular cartilage is typically 1-3 mm thick,[73, 74] the cartilage in the current study was only approximately 0.6 mm thick. Past studies

have shown that when diffusion through cartilage is substantially hindered, it is clearly observable in the first few hundred μm,[26, 36, 39] whereas our copolymers exhibited relatively uniform distribution across the explants. However, it is possible that the higher thickness of human cartilage would lead to a decreased depth of uptake of the cationic molecules. On the other hand, cyclic cartilage loading taking place *in vivo* may also facilitate uptake.[75] As such, further studies will be required to evaluate the translational potential of these cationic polymers.

Polycation cytotoxicity to bovine chondrocytes

As one of the relevant cell types that would be exposed to the polycations upon their intra-articular injection and the target cell following their uptake into cartilage, chondrocytes were selected for cytotoxicity testing. Chondrocytes were isolated from excised bovine articular cartilage following sequential enzymatic digestion with Pronase® protease and collagenase type I, expanded by two-dimensional culture, and used at passage two. The chondrocytes were treated with the polycations at concentrations of 0.125, 0.25, 0.5, or 1 mg/mL for 24 h. Cytotoxicity was evaluated using a 3-(4,5-dimethylthiazol-2-yl)-2,5-diphenyltetrazolium bromide (MTT) colorimetric assay. Overall, metabolic activity was highest following exposure to the most dilute polycation solutions (Fig. 7). In addition, with the exception of the ultra-high DP linear polycation and the highest concentrations of the high and ultra-high DP 8-arm polycation, the copolymers were generally well tolerated by the chondrocytes (60-89% cell viability compared to control). Based on ISO 10093-5, cell viability above 80% can be considered as non-cytotoxic, while 60 – 80% is considered to be weak cytotoxicity.[76] The high and ultra-high DP 8-arm polycations were better tolerated at lower concentrations. However, the ultra-high DP linear polymer was notably more toxic than the other polycations, even at lower concentrations.

The cytotoxicity of polycations at high concentrations is well established, and was also observed for other cartilage-penetrating systems such as the partially PEGylated PAMAM dendrimers[38] and IGF-1 complexes.[37] While not fully understood, the mechanism for polycationic macromolecules leading to cell death is proposed to involve membrane disruption by a surfactant[77] or phospholipid hydrolysis[78] mechanism. It was reported that increasing molar mass and charge density led to increased toxicity for a series of well-defined PEI and PLL-based polycations, likely due to their enhanced interactions with membranes.[79] For poly(2-(dimethylamino)ethyl methacrylate) star polymers, at a given molar mass, decreasing toxicity was observed with increasing number of arms from linear to 5-arm polymers.[80] It was proposed that not all amines in a star polymer, particularly those at the core, were able to participate in interactions with the cell membrane. Thus, our results are in line with those previously reported for the cytotoxicity of polycations. It should also be noted that the tested concentrations were high compared to what would be used in practice, and as much of the polymer would interact with the ECM *in vivo*, only a fraction would reach the cells, resulting in low local concentrations. Given these reflections, our interpretation of these results is that most polymers were well tolerated by chondrocytes at relatively high concentrations. Of course, assessment with other cell lines *in vitro* as well as *in vivo* studies will eventually be required to further assess the biocompatibility of these polymers, or ideally degradable analogues that would be cleared readily from the tissues after delivery of their cargo.

Conclusions

A library of poly(HPMA-*r*-APMA) polycations with varying DP (low, medium, high, and ultra-high) and well-defined architectures (linear, 4-arm and 8-arm) were successfully synthesized through RAFT polymerization and their uptake and retention in excised bovine articular cartilage was studied. We found that regardless of the presence of serum, in general the uptake and retention increased with the DP due to stronger multivalent electrostatic interactions. Modest decreases in uptake were observed for the ultra-high DP polycations in a few cases, likely due to transport within cartilage being hindered. In terms of architecture, the linear polymers exhibited higher uptake and retention than 4-arm or 8-arm analogues of similar overall DP. This trend can be attributed to the enhanced binding of the linear polycations to anionic aggrecans in cartilage. While charges near the core of multi-arm structures may be somewhat inaccessible for binding, the linear structures exhibit full conformational flexibility to maximize electrostatic binding. In general, the polycations were well tolerated by bovine chondrocytes, although cell viability was notably reduced for the ultra-high DP linear polycation and 1 mg/mL concentrations of the high and ultra-high DP 8-arm polycations. Again, these trends likely relate to the number of cations on the polymer and their availability for electrostatic interaction with the cell membrane. Considering the importance of balancing cartilage uptake and cytotoxicity, our results suggest that a linear polymer with an M_n of about 50 kg/mol (DP ~300) can serve as a suitable polymeric delivery vehicle for cartilage. Although we did not investigate different ratios of neutral/cationic monomers, a 3:1 ratio was reasonable in terms of allowing for polymer uptake without an excessively high cationic charge density which may hinder cartilage penetration. Finally, our poly(HPMA-*r*-APMA) copolymers provide the advantage of having many primary amines that can be modified to conjugate therapeutics (~70 for the high DP linear polycation). However, the methacrylamide backbone, while ideal to enable controlled polymerization, is not biodegradable. It would be advantageous to translate these current findings to a biodegradable polymer backbone before proceeding to validate uptake and drug delivery to cartilage *in vivo*.

Experimental

Procedures for the polymer synthesis are provided in the electronic supporting information.

Evaluation of polycation uptake in cartilage explants

Full thickness bovine articular cartilage was excised aseptically from the metacarpophalangeal joints of 2-4 years old animals sourced from a local abattoir (Tom Henderson Meats and Abattoir Inc., Ottawa, ON, Canada) within 24 h of death. Discs (6 mm diameter with the average mass of 26 ± 6 mg and the typical thickness of ~0.6 mm) were prepared from the excised cartilage samples using Miltex disposable biopsy punches (Integra) and used on the same day. Explanted cartilage discs were weighed and then incubated in 750 µL of Dulbecco's Modified Eagle Medium (DMEM; 4.5 g/L glucose; Corning, USA) without phenol red but supplemented with 100 U/mL of penicillin, 100 µg/mL streptomycin, and 250 µg/mL amphotericin B (1% v/v antibiotic-antimycotic solution, Sigma-Aldrich, Oakville, ON, Canada) and 10 µM of rhodamine-labelled polycations in a 48-well plate. The cartilage discs were incubated in the polycation-containing medium for 12 h on an orbital rocker at 37 °C in an environment comprising 5% CO_2 and greater than 95% relative humidity. Wells without cartilage discs were also prepared and incubated identically to allow any non-cartilage-mediated reductions in fluorescence to be accounted for. Blank solutions comprising medium alone without the addition of any polycations (and with or without a cartilage explant disc) were also evaluated to ensure that cartilage alone did not lead to any changes in fluorescence (no significant fluorescence was observed). After the incubation period, the fluorescence emission intensities in relative fluorescence units (RFU) of the solutions were measured at 590 nm using an excitation wavelength of 540 nm using a Synergy H1 microplate reader (BioTek). Polycation uptake was evaluated using the following equation:

$$\%\ \text{Uptake} = \frac{(\text{RFU}_{\text{PCM}} - \overline{\text{RFU}}_{\text{blank}}) - (\text{RFU}_{\text{PCM with explant}} - \overline{\text{RFU}}_{\text{blank}})}{\text{RFU}_{\text{PCM}} - \overline{\text{RFU}}_{\text{blank}}} \times 100\%$$

where PCM = polycation medium.

The experiment was repeated using all of the same methods, except that 5% v/v fetal bovine serum (FBS) was included in the culture medium. For each condition, the polycation uptake was evaluated in biological replicate (n=5) measurements and the results are reported as the mean ± standard deviation.

Evaluation of polycation retention in cartilage explants

A subset of cartilage explants were subsequently briefly rinsed three times in phosphate buffered saline (PBS, Sigma-Aldrich, Oakville, ON, Canada) and incubated in the fresh serum-free medium without the polycations for 48 h on an orbital rocker at 37 °C in an environment comprising 5% CO_2 and greater than 95% relative humidity to evaluate the release of polycations into the solution and calculate retention within cartilage. Fresh serum-free medium incubated in absence of cartilage explants served as blanks and with cartilage explants previously incubated in medium without polycations served as controls. Polycation retention was evaluated using the following equations:

$$\%\ \text{Release} = \frac{\text{RFU}_{\text{explant previously exposed to PCM}} - \overline{\text{RFU}}_{\text{blank}}}{\text{RFU}_{\text{expected signal of complete release}}} \times 100\%$$

$$\text{RFU}_{\text{expected signal of complete release}} = (\text{RFU}_{\text{PCM}} - \overline{\text{RFU}}_{\text{blank}}) -$$

$$(\text{RFU}_{\text{explant in PCM}} - \overline{\text{RFU}}_{\text{blank}})$$

$$\%\ \text{Retention} = \%\ \text{Uptake} - \%\ \text{Release}$$

The experiment was repeated using all of the same methods, except that 5% v/v fetal bovine serum (FBS) was included in the culture medium. The experiments were performed in biological triplicates and the results are presented as the mean ± standard deviation.

Fluorescence microscopy of cartilage explants after polycation uptake

Following incubation of the cartilage explants with the polycations, remaining explants (n = 2) not used for the evaluation of polycation retention were briefly rinsed three times in PBS and then sectioned into thin slabs (213±18 µm) using a custom-made device comprising a number 22 scalpel blade and a cryotome blade. The tissues were imaged immediately after sectioning for fluorescence distribution through the cross-section using an Axio Observer 7 microscope (Zeiss). Fluorescence profiles of the cartilage cross-sections were then evaluated using ZEN software (Zeiss; version 3.2).

Evaluation of polycation cytotoxicity in bovine chondrocytes

To isolate chondrocytes, bovine articular cartilage excised as described previously was first maintained in DMEM supplemented with 1% v/v antibiotic-antimycotic solution for 3 days to ensure the absence of contamination. The tissue pieces were then sequentially digested with 0.2% w/v Pronase® protease (EMD Millipore, Billerica, MA, USA) in DMEM for 2 h and 0.1% w/v collagenase type I (Sigma-Aldrich, Oakville, ON, Canada) in DMEM for 1 day. Following digestion, the cell suspension was pelleted by centrifugation at 500 rcf for 5 min, the supernatant removed, and chondrocytes resuspended in fresh DMEM. The washing steps were repeated three times. After the last wash, the chondrocytes were resuspended in DMEM supplemented with 5% v/v FBS and 1% v/v antibiotic-antimycotic solution and seeded in T175 flasks at 11,000 cells per cm^2 for expansion culture. Cells were passaged at 90% confluence and passage 2 chondrocytes were used for cytotoxicity tests.

For the assay, 5 x 104 chondrocytes per well were seeded onto 96-well plates in 100 µL of medium supplemented with 5% v/v FBS and 1% v/v antibiotic-antimycotic. The plates were incubated overnight at 37 °C in an environment comprising 5% CO2 and greater than 95% relative humidity to allow for cell attachment. The culture medium was then replaced with 100 µL of fresh medium supplemented with 5% v/v FBS and 1% v/v antibiotic-antimycotic solution containing 0.125 to 1 mg/mL of the polycations and incubated for 24 h. Cells cultured in medium without polycations were used as controls and wells containing the medium without cells served as blanks. After the incubation, the medium was replaced with 75 µL of fresh medium without polymer and 7.5 µL of 12 mM 3-(4,5-dimethylthiazol-2-yl)-2,5-diphenyltetrazolium bromide (MTT,

Sigma-Aldrich, CA) in sterile PBS was added to each well. After incubation for 4 h, 165 µL of dimethyl sulfoxide (DMSO; Sigma-Aldrich, CA) was added to each well and the plate was incubated for an additional 10 min at 37 °C. Each well was then thoroughly mixed, and absorbance was read at 540 nm using a Synergy H1 microplate reader. The mean absorbance of blank wells was subtracted from absorbance readings for each sample and the absorbance for wells containing cells but no polycation were considered as 100% metabolic activity for normalization of the data. Each polycation concentration was evaluated in triplicates and the data are presented as the mean ± standard deviation.

Histology

Full thickness articular cartilage was excised to incorporate subchondral bone, washed 3-times with PBS and fixed for 72h with 10% v/v formalin. Samples were then decalcified in 0.5 M Ethylenediaminetetraacetic acid (EDTA) for 1 month, before being embedded in paraffin. The blocks were sectioned to 4 µm and mounted on slides. The sections were stained with Safranin-O and counterstained with Nuclear Fast Red. The sections were then imaged with a Zeiss AxioScan Z1 Slide Scanner

Author Contributions

Jue Gong: methodology, formal analysis, investigation, writing – original draft. Jordan Nhan: methodology, formal analysis, investigation, writing – review & editing. Jean-Philippe St-Pierre: methodology, investigation, supervision, funding acquisition, writing – review & editing. Elizabeth R. Gillies: conceptualization, methodology, supervision, funding acquisition, writing – review & editing.

Conflicts of interest

The authors declare no competing financial interest.

Acknowledgements

We thank the Natural Sciences and Engineering Research Council of Canada (ERG: RGPIN 2021-03950; JPS: RGPIN 2017-04593) for funding. ERG thanks the Canada Research Chairs program (CRC-2020-00101). JPS was supported by a Stars Career Development Award from the Arthritis Society Canada [STAR-19-0606; 2020-2022] with matching funds from the Canadian Institutes of Health Research. Some instruments used in the study were acquired with funds from the Canadian Foundation for Innovation [JPS: CFI-37732; 2020-2022] with matching funds from the Ministry of Economic Development, Job Creation and Trade Ontario Research Fund. Aneta Borecki is acknowledged for assistance with SEC analyses. The Louise Pelletier Histology Core facility at the University of Ottawa (RRID: SCR_021737) is acknowledged for the preparation of a histological image.

Notes and references

1 H. Long, Q. Liu, H. Yin, K. Wang, N. Diao, Y. Zhang, J. Lin and A. Guo, *Arthritis Rheumatol.*, 2022, **74**, 1172-1183.
2 S. Safiri, A. A. Kolahi, E. Smith, C. Hill, D. Bettampadi, M. A. Mansournia, D. Hoy, A. Ashrafi-Asgarabad, M. Sepidarkish, A. Almasi-Hashiani, G. Collins, J. Kaufman, M. Qorbani, M. Moradi-Lakeh, A. D. Woolf, F. Guillemin, L. March and M. Cross, *Ann. Rheum. Dis.*, 2020, **79**, 819-828.
3 S. Glyn-Jones, A. J. R. Palmer, R. Agricola, A. J. Price, T. L. Vincent, H. Weinans and A. J. Carr, *Lancet*, 2015, **386**, 376-387.
4 M. J. Richard, J. B. Driban and T. E. McAlindon, *Osteoarthritis Cartilage*, 2023, **31**, 458-466.
5 M. Choueiri, X. Chevalier and F. Eymard, *Cartilage*, 2021, **13**, 122s-131s.
6 D. Webner, Y. Huang and C. D. Hummer, 3rd, *Cartilage*, 2021, **13**, 1619s-1636s.
7 A. J. Carr, O. Robertsson, S. Graves, A. J. Price, N. K. Arden, A. Judge and D. J. Beard, *Lancet*, 2012, **379**, 1331-1340.
8 R. Pivec, A. J. Johnson, S. C. Mears and M. A. Mont, *Lancet*, 2012, **380**, 1768-1777.
9 A. Latourte, M. Kloppenburg and P. Richette, *Nat. Rev. Rheumatol.*, 2020, **16**, 673-688.
10 P. Krzeski, C. Buckland-Wright, G. Bálint, G. A. Cline, K. Stoner, R. Lyon, J. Beary, W. S. Aronstein and T. D. Spector, *Arthritis Res. Ther.*, 2007, **9**, R109.
11 E. M. van der Aar, J. Desrivot, L. Fagard, D. Amantini, S. Larsson, A. Struglics, S. Lohmander, F. Vanhoutte and S. Dupont, *Osteoarthritis Cartilage*, 2018, **26**, S310.
12 E. van der Aar, H. Deckx, M. Van Der Stoep, M. Wooning, K. Bernard, S. Grankov, O. Imbert, M. Pueyo and F. Eckstein, *Osteoarthritis Cartilage*, 2020, **28**, S499-S500.
13 M. Karsdal, M. Michaelis, C. Ladel, A. Siebuhr, A. Bihlet, J. Andersen, H. Guehring, C. Christiansen, A. Bay-Jensen and V. Kraus, *Osteoarthritis Cartilage*, 2016, **24**, 2013-2021.
14 M. C. Hochberg, A. Guermazi, H. Guehring, A. Aydemir, S. Wax, P. Fleuranceau-Morel, A. Reinstrup Bihlet, I. Byrjalsen, J. R. Andersen and F. Eckstein, *JAMA*, 2019, **322**, 1360-1370.
15 P. Maudens, O. Jordan and E. Allemann, *Drug Discov. Today*, 2018, **23**, 1761-1775.
16 S. Mehta, T. He and A. G. Bajpayee, *Curr. Opin. Rheumatol.*, 2021, **33**, 94-109.
17 L. M. Mancipe Castro, A. J. García and R. E. Guldberg, *J. Biomed. Mater. Res. A*, 2021, **109**, 426-436.
18 C. H. Evans, V. B. Kraus and L. A. Setton, *Nat. Rev. Rheumatol.*, 2014, **10**, 11-22.
19 C. Larsen, J. Ostergaard, S. W. Larsen, H. Jensen, S. Jacobsen, C. Lindegaard and P. H. Andersen, *J. Pharm. Sci.*, 2008, **97**, 4622-4654.
20 B. C. Geiger, A. J. Grodzinsky and P. T. Hammond, *Chem. Eng. Prog*, 2018, **114**, 46-51.
21 C. D. DiDomenico and L. J. Bonassar, *Osteoarthritis Cartilage*, 2018, **26**, 1438-1446.
22 X. Mei, I. J. Villamagna, T. Nguyen, F. Beier, C. T. Appleton and E. R. Gillies, *Biomed. Mater.*, 2021, **16**, 042006.
23 S. Brown, S. Kumar and B. Sharma, *Acta Biomater.*, 2019, **93**, 239-257.
24 Z. He, B. Wang, C. Hu and J. Zhao, *Colloids Surf. B Biointerfaces*, 2017, **154**, 33-39.
25 A. Gupta, J. Lee, T. Ghosh, V. Q. Nguyen, A. Dey, B. Yoon, W. Um and J. H. Park, *Pharmaceutics*, 2022, **14**, 540.
26 A. G. Bajpayee, C. R. Wong, M. G. Bawendi, E. H. Frank and A. J. Grodzinsky, *Biomaterials*, 2014, **35**, 538-549.
27 C. Sacchetti, R. Liu-Bryan, A. Magrini, N. Rosato, N. Bottini and M. Bottini, *ACS Nano*, 2014, **8**, 12280-12291.
28 D. A. Rothenfluh, H. Bermudez, C. P. O'Neil and J. A. Hubbell, *Nat. Mater.*, 2008, **7**, 248-254.

29 Y. Pi, X. Zhang, J. Shi, J. Zhu, W. Chen, C. Zhang, W. Gao, C. Zhou and Y. Ao, *Biomaterials*, 2011, **32**, 6324-6332.
30 X. Ai, Y. Duan, Q. Zhang, D. Sun, R. H. Fang, W. Gao, L. Zhang and R. Liu-Bryan, *Bioeng. Transl. Med.*, 2021, **6**, e10187.
31 A. G. Bajpayee and A. J. Grodzinsky, *Nat. Rev. Rheumatol.*, 2017, **13**, 183-193.
32 A. G. Bajpayee, M. Scheu, A. J. Grodzinsky and R. M. Porter, *J. Orthop. Res.*, 2014, **32**, 1044-1051.
33 A. G. Bajpayee, M. Scheu, A. J. Grodzinsky and R. M. Porter, *J. Orthop. Res.*, 2015, **33**, 660-667.
34 T. He, C. Zhang, A. Vedadghavami, S. Mehta, H. A. Clark, R. M. Porter and A. G. Bajpayee, *J. Controlled Release*, 2020, **318**, 109-123.
35 T. He, I. Shaw, A. Vedadghavami and A. G. Bajpayee, *Cartilage*, 2022, **13**, 19476035221093072.
36 Y. Krishnan, H. A. Rees, C. P. Rossitto, S. E. Kim, H. K. Hung, E. H. Frank, B. D. Olsen, D. R. Liu, P. T. Hammond and A. J. Grodzinsky, *Biomaterials*, 2018, **183**, 218-233.
37 N. J. Shah, B. C. Geiger, M. A. Quadir, M. N. Hyder, Y. Krishnan, A. J. Grodzinsky and P. T. Hammond, *Bioeng. Transl. Med.*, 2016, **1**, 347-356.
38 B. C. Geiger, S. Wang, R. F. Padera Jr., A. J. Grodzinsky and P. T. Hammond, *Sci. Transl. Med.*, 2018, **10**, eaat8800.
39 A. Vedadghavami, E. K. Wagner, S. Mehta, T. He, C. Zhang and A. G. Bajpayee, *Acta Biomater.*, 2019, **93**, 258-269.
40 J. M. Ren, T. G. McKenzie, Q. Fu, E. H. Wong, J. Xu, Z. An, S. Shanmugam, T. P. Davis, C. Boyer and G. G. Qiao, *Chem. Rev.*, 2016, **116**, 6743-6836.
41 G. Moad, E. Rizzardo and S. H. Thang, *Chem. – Asian J.*, 2013, **8**, 1634-1644.
42 D. J. Keddie, G. Moad, E. Rizzardo and S. H. Thang, *Macromolecules*, 2012, **45**, 5321-5342.
43 A. Ghamkhari, B. Massoumi and S. Agbolaghi, *Polym. Int.*, 2018, **67**, 283-291.
44 P. van de Wetering, A. T. Metters, R. G. Schoenmakers and J. A. Hubbell, *J. Controlled Release*, 2005, **102**, 619-627.
45 J. W. DuBose, C. Cutshall and A. T. Metters, *J. Biomed. Mater. Res. A*, 2005, **74**, 104-116.
46 R. G. Schoenmakers, P. van de Wetering, D. L. Elbert and J. A. Hubbell, *J. Controlled Release*, 2004, **95**, 291-300.
47 J. Kopecek and P. Kopecková, *Adv. Drug Deliv. Rev.*, 2010, **62**, 122-149.
48 R. Duncan and M. J. Vicent, *Adv. Drug Deliv. Rev.*, 2010, **62**, 272-282.
49 P. Chytil, L. Kostka and T. Etrych, *J. Pers. Med.*, 2021, **11**, 115.
50 R. M. Kleinberger, N. A. Burke, C. Zhou and H. D. Stöver, *J. Biomater. Sci. Polym. Ed.*, 2016, **27**, 351-369.
51 L. C. Paslay, B. A. Abel, T. D. Brown, V. Koul, V. Choudhary, C. L. McCormick and S. E. Morgan, *Biomacromolecules*, 2012, **13**, 2472-2482.
52 P. I. Kitov, E. Paszkiewicz, J. M. Sadowska, Z. Deng, M. Ahmed, R. Narain, T. P. Griener, G. L. Mulvey, G. D. Armstrong and D. R. Bundle, *Toxins*, 2011, **3**, 1065-1088.
53 S. C. Larnaudie, J. C. Brendel, K. A. Jolliffe and S. Perrier, *ACS Macro Lett.*, 2017, **6**, 1347-1351.
54 L. Fetters, N. Hadjichristidis, J. Lindner and J. Mays, *J. Phys. Chem. Ref. Data*, 1994, **23**, 619-640.
55 O. Lidický, M. Šírová and T. Etrych, *Physiol. Res.*, 2016, **65**, S233-S241.
56 J. Jennings, M. Beija, J. T. Kennon, H. Willcock, R. K. O'Reilly, S. Rimmer and S. M. Howdle, *Macromolecules*, 2013, **46**, 6843-6851.
57 S. Allison-Logan, F. Karimi, Y. Sun, T. G. McKenzie, M. D. Nothling, G. Bryant and G. G. Qiao, *ACS Macro Lett.*, 2019, **8**, 1291-1295.
58 H. Chaffey-Millar, M. H. Stenzel, T. P. Davis, M. L. Coote and C. Barner-Kowollik, *Macromolecules*, 2006, **39**, 6406-6419.
59 D. Pissuwan, C. Boyer, K. Gunasekaran, T. P. Davis and V. Bulmus, *Biomacromolecules*, 2010, **11**, 412-420.
60 T. Nguyen and M. B. Francis, *Org. Lett.*, 2003, **5**, 3245-3248.
61 A. Vedadghavami, T. He, C. Zhang, S. M. Amiji, B. Hakim and A. G. Bajpayee, *Acta Biomater.*, 2022, **151**, 278-289.
62 J. D. Freedman, H. Lusic, B. D. Snyder and M. W. Grinstaff, *Angew. Chem. Int. Ed.*, 2014, **53**, 8406-8410.
63 H.-Y. Hu, N.-H. Lim, H.-P. Juretschke, D. Ding-Pfennigdorff, P. Florian, M. Kohlmann, A. Kandira, J. P. Von Kries, J. Saas and K. A. Rudolphi, *Chem. Sci.*, 2015, **6**, 6256-6261.
64 D. A. Rothenfluh, H. Bermudez, C. P. O'Neil and J. A. Hubbell, *Nat. Mater.*, 2008, **7**, 248-254.
65 W. D. Comper, eds. B. K. Hall and S. A. Newman, CRC Press, Boston, 1991, pp. 59-96.
66 L. Ng, A. J. Grodzinsky, P. Patwari, J. Sandy, A. Plaas and C. Ortiz, *J. Struct. Biol.*, 2003, **143**, 242-257.
67 A. Maroudas, *J. Anat.*, 1976, **122**, 335-347.
68 H. G. Rennke and M. A. Venkatachalam, *J. Clin. Invest.*, 1979, **63**, 713-717.
69 M. P. Bohrer, W. M. Deen, C. R. Robertson, J. L. Troy and B. M. Brenner, *J. Gen. Physiol.*, 1979, **74**, 583-593.
70 E. R. Gillies, E. Dy, J. M. Fréchet and F. C. Szoka, *Mol. Pharm.*, 2005, **2**, 129-138.
71 G. I. Im, *Tissue Eng. Regen. Med.*, 2022, **19**, 431-436.
72 S. Brown, J. Pistiner, I. M. Adjei and B. Sharma, *Mol. Pharm.*, 2017, **16**, 469-479.
73 C. Adam, F. Eckstein, S. Milz and R. Putz, *J. Anat.*, 1998, **193**, 203-214.
74 D. Shepherd and B. Seedhom, *Ann. Rheum. Dis.*, 1999, **58**, 27-34.
75 H. Meng, Q. Quan, X. Yuan, Y. Zheng, J. Peng, Q. Guo, A. Wang and S. Lu, *J. Orthop. Translat.*, 2020, **22**, 58-66.
76 Tests for In Vitro Cytotoxicity, in *Biological Evaluation of Medical Devices*, ISO, Geneva, 2009, 10993-5.
77 S. Vaidyanathan, B. G. Orr and M. M. Banaszak Holl, *Acc. Chem. Res.*, 2016, **49**, 1486-1493.
78 A. M. Seddon, D. Casey, R. V. Law, A. Gee, R. H. Templer and O. Ces, *Chem. Soc. Rev.*, 2009, **38**, 2509-2519.
79 B. D. Monnery, M. Wright, R. Cavill, R. Hoogenboom, S. Shaunak, J. H. G. Steinke and M. Thanou, *Int. J. Pharm.*, 2017, **521**, 249-258.
80 C. V. Synatschke, A. Schallon, V. Jérôme, R. Freitag and A. H. Müller, *Biomacromolecules*, 2011, **12**, 4247-4255.

